Street-Specific Handover Optimization for Vehicular Terminals in Future Cellular Networks

Zhe Ren*, Peter Fertl*, Qi Liao†, Federico Penna† and Sławomir Stańczak†
*BMW Forschung und Technik, Hanauerstrasse 46, Munich, Germany
Email: {zhe.ren, peter.fertl}@bmw.de
†Fraunhofer Institute for Telecommunications Heinrich Hertz Institute, Einsteinufer 37, Berlin
Email: {qi.liao,federico.penna,slawomir.stanczak}@hhi.fraunhofer.de

***Abstract*—Modern vehicles will have strong requirements with regard to seamless mobility support in future cellular systems, in order to enable advanced cooperative driver assistance and infotainment systems that guarantee traffic safety and efficiency. In this work, we introduce street-specific handover parameters for vehicular terminals. In particular, we propose an adaptive optimization algorithm that exploits vehicle context information in order to tune the handover parameters. Simulation results confirm that the proposed concept has the potential to improve handover performance significantly.**

I. Introduction

Optimization of cellular communication systems is crucial for delivering high quality services in legacy networks like Global System for Mobile Communications (GSM), Universal Mobile Telecommunications System (UMTS), etc [1]. In this context, Self-Organizing Network (SON) has been a part of Long Term Evolution (LTE) since 3GPP Release 9 as a key enhancement for improving Operations & Maintenance (O&M) by means of automated system control [2].One important concept of SON is Mobility Robustness Optimization (MRO), which intends to guarantee proper terminal mobility by automatically optimizing the handover performance.

Although the relevant handover Key Performance Indicator (KPI)s (e.g., Radio Link Failure (RLF) and Handover Ping-Pong Rate (HPR)) can be controlled by several parameters (e.g., Time to Trigger (TTT) and Handover Offset Margin (HOM)), it is difficult to determine their dependences analytically. For this reason several MRO algorithms have been proposed that adaptively minimize a certain KPI [3][4] or a set of KPIs [5][6] by adjusting the relevant control parameters.

Network-wide handover optimization based on a global parameter set represents a suboptimal solution, since it does not take into account individual user profiles such as mobility pattern, Quality of Service (QoS) or radio conditions. Therefore, this approach only achieves promising results when one type of user profile dominates the network or the current cell, which will not be the case in future heterogeneous cellular systems. Consequently, user-specific optimization represents the best solution, but is considered to be unrealistic [7]. However, particular user context information such as velocity may influence the handover performance significantly [8], [7]. Therefore, mobility dependent parameter scaling has been specified in the Radio Resource Control (RRC) protocol of 3GPP LTE [9]. Many modern vehicles are already equipped with advanced cellular communication terminals (e.g., based on UMTS and LTE). In order to enable reliable cooperative driver assistance services that improve traffic safety and efficiency in the future, seamless mobility support for vehicular terminals is required. to guarantee these requirements enhanced mobility support for vehicular terminals is required. applications from on-board units to off-board, backend components. We therefore propose to use street-specific handover parameters to enhance the handover performance of vehicular terminals. In contrast to conventional user terminals that behave strongly non-stationary, vehicular terminals move along a defined path (i.e., streets) and within a certain speed range. Moreover, the position and trajectory of vehicles is usually well known due to on-board Global Positioning System (GPS) and navigation systems. Thus, handover decisions can be improved based on this additional information.

In this paper, we derive a suitable optimization algorithm and show the handover performance gains that are achieved by exploiting street-specific context information such as speed limit, road direction and corresponding radio propagation characteristics. Results confirm that the proposed concept and algorithm yield significant gains in comparison with cell-pair specific optimization, even if in both approaches the terminals cross the cell boundaries with the same speed.

The rest of the paper is organized as follows: **??** the LTE handover process and the underlying system model is reviewed. In Section II, the street specific handover parameter optimization problem is formulated. handover optimization is described in Section . A heuristic optimization algorithm based on the estimated handover performance is proposed in Section III and simulation results are shown in Section IV. Finally, conclusions are drawn in the last section.

II. Problem Statement

A. LTE Handover Process

In LTE wireless networks, a User Equipment (UE) assisted handover process is specified for intra Evolved-UMTS Ter-

[1]Part of this work has been performed in the framework of the FP7 project ICT-317669 METIS, which is partly funded by the European Union. The authors would like to acknowledge the contributions of their colleagues in METIS, although the views expressed are those of the authors and do not necessarily represent the project.

restrial Radio Access Network (E-UTRAN) handovers [9]. When the Reference Signal Received Power (RSRP) from neighboring evolved Node B (eNB) becomes offset better than serving eNB, the event "A3" is entered. A handover request is triggered if the A3 condition holds for a certain time TTT. For simplicity in this study, we refer to HOM as the sum of handover offset and any other specific offsets.

While sufficiently large values of HOM and TTT are necessary to reduce/limit the total number of handovers, these values need to be small enough to reduce the number of RLFs. This suggests that HOM and TTT must be chosen so as to find a desired tradeoff between different handover KPIs that in general contradict each other and therefore cannot be minimized at the same time. For the rest of the paper, we use H and T to denote HOM and TTT, respectively. Moreover, we assume the network to be symmetric, so that eNBs have the same set of H and T.

B. Handover KPI

The handover KPIs of interest in this paper are the observed channel outage ratio denoted by R_{out} and the handover ping-pong ratio designated by R_{pp}. Both ratios can be measured and collected at eNBs as follows:

$$R_{\text{out}} = \frac{N_{\text{outslots}}}{N_{\text{slots}}} \tag{1}$$

$$R_{\text{pp}} = \frac{N_{\text{pp}}}{N_{\text{ho}}} \tag{2}$$

Here, N_{slots} denotes the total number of the counting time slots after the occurrence of an A3 event, and N_{outslots} refers to the number of time slots which do not support a minimum SINR requirement Γ_{min} within the total counting time slots. In 2,N_{pp} and N_{ho} denote the number of observed ping-pong handover events and the number of handover events from one eNB to another, respectively.

C. Problem Statement

As indicated in Section (II-A), there is a trade-off between R_{out} and R_{pp} so that in general one of the objectives can only be minimized at the cost of the other. This is a typical multivariate multi-objective optimization problem. A widely-used approach to multi-objective optimization problems is to minimize one of the objectives while constraining all other objectives to some predefined target values. In our case, the problem takes the following form:

$$\begin{aligned} \underset{\boldsymbol{\theta}}{\text{minimize}} \quad & R_{\text{out}}(\boldsymbol{\theta}) \\ \text{subject to} \quad & R_{\text{pp}}(\boldsymbol{\theta}) \leq R_{\text{t}} \end{aligned} \tag{3}$$

where R_{t} is the target ping-pong rate and $\boldsymbol{\theta}$ is a vector of handover parameters, including HOM and TTT of each street. With m streets we have $\boldsymbol{\theta} := (H_1, \ldots, H_m, T_1, \ldots, T_m)$.

Unfortunately, the problem in (3) cannot be addressed using standard optimization tools as the dependence of R_{out} and R_{pp} on the control parameters HOM and TTT is not known. Therefore, we propose using other optimization objectives based on probabilistic consideration.

III. Street-Specific Handover Optimization

A. Optimization Objectives

We define $\Delta^{(t)} = p_{\text{n}}^{(t)} - p_{\text{s}}^{(t)}$ to be the difference at the t-th time unit between the RSRP in the neighboring target cell (subscript n) and the serving cell (subscript s). Consequently, the A3 Event is entered when $\Delta^{(t)} > H$ and, if this condition holds for time T, then a handover is triggered.

In this paper, the HO performance measures of interest R_{out} and R_{pp} are approximated by upper bounding some related probabilities that are denoted by P_{out} and P_{pp}. To introduce the probabilities, assume that the A3 event is triggered in time slot t_0, while the handover from a serving cell to a target cell occurs in time slot t_1. With this in hand, we define P_{out} during the time period $[t_0 + 1, t_0 + T]$ to be

$$P_{\text{out}}^{(t_0+T)} = \frac{1}{T}\sum_{\tau=1}^{T} Pr\{\text{SINR}^{(t_0+\tau)} < \Gamma_{\text{min}}\} \tag{4}$$

$$\approx \hat{P}_{\text{out}}^{(t_0+T)} = \frac{1}{T}\sum_{\tau=1}^{T} Pr\{-\Delta^{(t_0+\tau)} < \Gamma_{\text{min}}\} \tag{5}$$

while P_{pp} during the time period $[t_1 + 1, t_1 + T]$ is

$$P_{\text{pp}}^{(t_1+T)} = \prod_{\tau=1}^{T} Pr\{-\Delta^{(t_1+\tau)} > H\} \tag{6}$$

$$\approx \hat{P}_{\text{pp}}^{(t_1+T)} = \prod_{\tau=1}^{T} Pr\{-\Delta^{(t_0+T+\tau)} > H\}\,. \tag{7}$$

Note that (5) is a good approximation of (4) only if for cell edge users, the thermal noise and the overall interference from all cells except for the target cell are negligible when compared with the dominant interferer from the target cell.

From (5) and (7), we can see how the optimization objectives P_{out} and P_{pp} depend on the control parameters $\{H, T\}$ and the distribution of the RSRP difference Δ. As far as the distribution of $\Delta^{(t_0+\tau)}, \tau > 0$, in (5) is concerned, we have

$$\mu(\Delta^{(t_0+\tau)}) = H + M^{(t_0+\tau)} \tag{8}$$

$$\sigma(\Delta^{(t_0+\tau)}) = C \tag{9}$$

where $\mu(\Delta^{(t)})$ and $\sigma(\Delta^{(t)})$ are the mean and variance of $\Delta^{(t)}$, respectively. Note that $M^{(t_0+\tau)}$ depends on the mobility and the moving direction of the user, while C in (9) is a constant which may have to be learned by machine learning techniques. For more details about (8) and (9), the reader is referred to Appendix A. Similarly, the mean and the variance of $\Delta^{(t_0+T+\tau)}$ in (7) yield $\mu(\Delta^{(t_0+T+\tau)}) = H + M^{(t_0+T+\tau)}$ and $\sigma(\Delta^{(t_0+T+\tau)}) = C$, respectively.

The probabilities in (5) and (7) cannot be calculated explicitly since the distributions of the random variables are not known. Hence, we use the first two moments to derive the following upperbounds on P_{out} and P_{pp} (see Appendix B and C for more details)

$$\bar{P}_{\text{out}}^{(t_0+T)} = \frac{C}{2T}\sum_{\tau=1}^{T} \frac{1}{\left(H + M^{(t_0+\tau)} + \Gamma_{\text{min}}\right)^2} \tag{10}$$

$$\bar{P}_{\text{pp}}^{(t_1+T)} = \frac{C}{2}\prod_{\tau=1}^{T} \frac{1}{\left(2H + M^{(t_0+T+\tau)}\right)^2}\,. \tag{11}$$

These upperbounds are used in the optimization algorithm presented in the following section.

B. Adaptive Optimization Algorithm

By (10) and (11), the optimization objectives $\bar{P}_{\text{out}}^{(t_0+T)}$ and $\bar{P}_{\text{pp}}^{(t_1+T)}$ depends on the control parameter T and H as well as on $M^{(t_0+\tau)}$ given by (19) in appendix, which is a function of speed, direction and radio propagation. This fact is exploited in this paper to improve handover performance by introducing street-specific handover parameters. Based on $\bar{P}_{\text{out}}^{(t_0+T)}$ and $\bar{P}_{\text{pp}}^{(t_1+T)}$, we propose a heuristic algorithm for adjusting the street-specific handover parameters T and H. The approach is summarized in Algorithm 1. The idea is very simple: if the measured ping-pong rate is acceptable, the algorithm attempts to reduce $\bar{P}_{\text{out}}$ by decreasing that parameter which leads to the largest descent of $\bar{P}_{\text{out}}$. On the other hand, if the ping-pong rate exceeds the target, the algorithm tries to reduce $\bar{P}_{\text{pp}}$ by increasing H or T of the street with the largest descent of $\bar{P}_{\text{pp}}$. The notation used in the algorithm is defined as follows: the ith entry of $\boldsymbol{\theta}$ is denoted by θ_i, while $\Delta\theta_i$ is the corresponding resolution. During the handover process, it is assumed that $M^{(t_0+\tau)}$ is constant and equal to M such that $\bar{P}_{\text{out}}^{(t_0+T)} = \bar{P}_{\text{out}}(\theta_i)$ and $\bar{P}_{\text{pp}}^{(t_1+T)} = \bar{P}_{\text{pp}}(\theta_i), 1 \le i \le 2m$.

Algorithm 1: Street-Specific Parameter Optimization

initialization of $\boldsymbol{\theta} = [H_1, H_2, \ldots H_m, T_1, T_2, \ldots, T_m]$
set R_{t} as the targeting rate of R_{pp}
loop
  get $R_{\text{pp}}(\boldsymbol{\theta})$ under the current parameter set $\boldsymbol{\theta}$
  if $R_{\text{pp}}(\boldsymbol{\theta}) < R_{\text{t}}$ **then**
    while $R_{\text{pp}}(\boldsymbol{\theta}) < R_{\text{t}}$ **do**
      $i = \text{argmax}_i\{\bar{P}_{\text{out}}(\theta_i) - \bar{P}_{\text{out}}(\theta_i - \Delta\theta_i)\}$
      if $\bar{P}_{\text{out}}(\theta_i) - \bar{P}_{\text{out}}(\theta_i - \Delta\theta_i) > 0$ **then**
        $\theta_{i+1} = \theta_i - \Delta\theta_i$ and update R_{pp} and R_{out}
      else
        break
      end if
    end while
  else
    while $R_{\text{pp}}(\boldsymbol{\theta}) > R_{\text{t}}$ **do**
      $i = \text{argmax}_i\{\bar{P}_{\text{pp}}(\theta_i) - \bar{P}_{\text{pp}}(\theta_i + \Delta\theta_i)\}$
      if $\bar{P}_{\text{pp}}(\theta_i) - \bar{P}_{\text{pp}}(\theta_i + \Delta\theta_i) > 0$ **then**
        $\theta_{i+1} = \theta_i + \Delta\theta_i$ and update R_{pp} and R_{out}
      else
        break
      end if
    end while
  end if
end loop

IV. Simulations

A. Simulation Scenario

LTE conform simulations are carried out to evaluate the performance of the proposed algorithm and to show the potential improvement due to street-specific handover parameters. As listed in Table I, all the system parameters are selected according to the LTE recommendation. A network with three eNBs and 500 m Inter Site Distance (ISD) is considered. The interference from outer-tier eNBs are constant and treated as noise (5 dB). The simulations setup is shown in Fig.1, where vehicles are supposed to move from the serving eNB to the targeting eNB along the depicted streets. For each street, there is a speed limit and vehicles are assumed to move with $\pm 10\%$ uniform deviation of that speed limit.

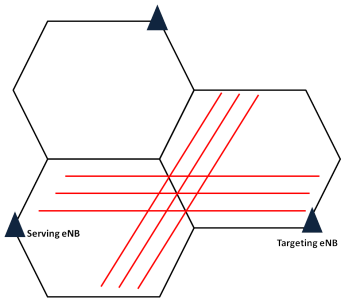

Fig. 1. street outline of the simulation scenarios

Scenarios with 2, 3 and 4 streets, which are chosen from 6 available streets as in Fig.1, are simulated and the results are the average of the gains achieved by all the combinations. Furthermore, the paper focuses on scenarios with the same speed profile for each street, because it has been discussed in [8] that handover parameters should be adjusted according to the terminal speed and we just focus on highlighting the additional improvement due to driving direction.

TABLE I
SIMULATION CONFIGURATIONS

System Parameters	
Pathloss in [dB]	$L = 128 + 37.6\,log_{10}(r)$ @ 2 GHz
eNB transmission power	46 dBm
eNB antenna pattern	$-\min(20, 12 \cdot (\frac{\theta}{\theta_{3dB}})^2)$, $\theta_{3dB} = 70°$
Terminal Noise figure	5 dB
Shadow fading	de-correlation distance 50 m, variance 8 dB
Fast Fading	IDFT implementation [10]
Handover Parameters	
In & Out of synch threshold	-4 dB & -6 dB
T310, N310 N311	500 ms, 1, 1
L3 filtering coefficient	2
Resolution of TTT & HOM	50 ms and 0.5 dB

B. Discussion

In order to evaluate the performance with street-specific handover parameter optimization, the following algorithms or theoretical optima are taken into account:

- Cell Pair Parameter Optimization (CPPO) with SON root cause optimization algorithm as in [3].
- Combinatorial optimum for CPPO by brute force.
- Street-Specific Parameter Optimization (SSPO) algorithm as proposed in Section III.
- Combinatorial optimum for SSPO by brute force.

A direct comparison between CPPO and SSPO can be found in Fig.2, where the speed limit of every street is set to 72 km/h and three streets are chosen. As can be seen, SSPO yields a

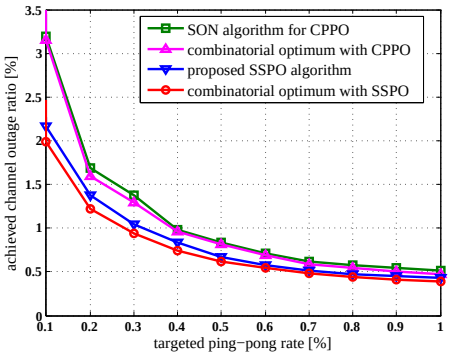

Fig. 2. Performance comparision of CCPO and SSPO

significantly better set of outage ratio when compared with CCPO. When the requirement on ping-pong rate is relatively stringent (e.g., 0.1%), more than 50% outage reduction can be expected. It is obviously that the proposed algorithm outperforms the SON algorithm for CCPO as well as its combinatorial optima. The results from the proposed SSPO algorithm are close to the optimal values achieved by brute force search, however, it must be emphasized that different initializations lead to different gains.

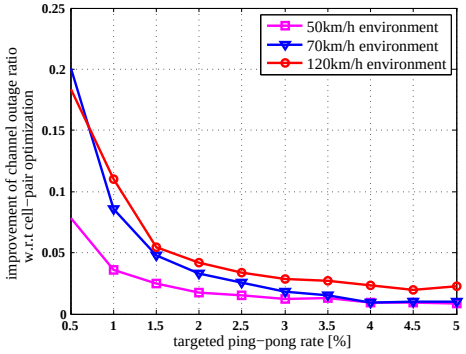

Fig. 3. Performance of SSPO depending on UE speed

In what follows, we further analyze the optimization problems by comparing simulation results of different UE speeds and different numbers of streets. In order to study the potential improvement, the comparison is based on the combinatorial optima. We denote R_{cp} and R_{ss} as the optimal outage ratio that can be achieved by CPPO and SPPO. In Fig.3, the reduction of channel outage ratio ($R_{\text{cp}} - R_{\text{ss}}$) is illustrated. Similar to the previous simulations, combinations of three streets are selected and the speeds environment for comparison are set to 50 km/h, 72 km/h and 120 km/h. It is obviously from the figure that higher gains are expected with higher speed and higher handover accuracy requirement. The reason why this occurred can be well explained by examining (19), where higher speed indicates higher mobility. The diversity of mobility profiles will be higher such that the optimal handover parameter set should be quite different on each street and single parameter could hardly accommodate the diversity.

In Fig.4, the outage reduction ($R_{\text{cp}} - R_{\text{ss}}$) is shown for different numbers of streets, where the speed limit is chosen as 72 km/h. We can conclude from the figure that cells connected by more streets will have more improvement due to SSPO,

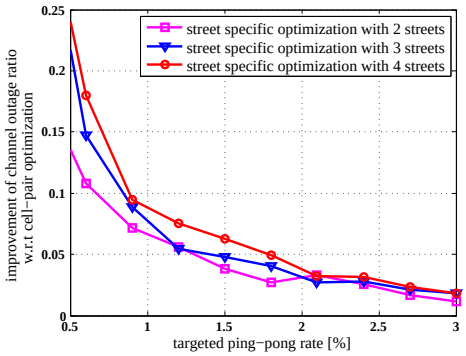

Fig. 4. Performance of SSPO depending on number of streets

since again, the large diversity of mobility profiles cannot be well addressed by a single cell pair parameter set. This means, the gain due to SSPO will be amplified in a real urban scenario with sophisticate street layouts and user mobility patterns.

V. Conclusion

In this paper, we introduced street-specific handover parameters to improve mobility management of the system. Evaluation results confirm that the handover performance in terms of channel outage ratio and ping-pong rate can be significantly improved with the proposed concept. Moreover, we have presented a first approach of an adaptive optimization algorithm that determines the street-specific parameters by exploiting street and terminal specific context information such as speed limit, road direction as well as the corresponding radio propagation characteristics. Under certain conditions the proposed algorithm has the potential to achieve close-to-optimal performance. More detailed investigations of the robustness of the proposed algorithm under various network conditions are considered in a future work.

Appendix

A. Physical Layer Measurement

In an LTE network, the received signal strength of a UE in logarithm domain can be expressed as:

$$p^{(t)} = y^{(t)} + \psi^{(t)} = p_{\text{t}} + l^{(t)} + g^{(t)} + \psi^{(t)} \tag{12}$$

where

$$l^{(t)} = A_1 + A_2 \log_{10}(r^{(t)}) \tag{13}$$

$$g^{(t)} = -B_1\left(\beta^{(t)}/B_2\right)^2 \tag{14}$$

where p_{t} is eNB transmission power. The path loss $l^{(t)}$ and the total antenna gain $g^{(t)}$ depend on the distance r between eNB and UE, and on the azimuth of the current location β. The constants A_1 and A_2 are the path loss reference and the path loss exponent, respectively, while B_1 and B_2 denote the attenuation constant and the 3-dB beamwidth respectively. The fading $\psi^{(t)}$ comprises shadowing and fast fading, which are typically modeled as Log-normal distributed and Rayleigh distributed random variables, respectively. Suppose that a user follows the uniform velocity rectilinear motion with fixed speed v_0 and moving direction (to antenna boresight) α_0. Its movement trajectory is shown in Fig.5. Assume that the measurements for distance r and azimuth β at time $t_i > 0$

are r_i and β_i respectively. Define $\Delta x^{(t_i)} := \frac{x^{(t_i+\Delta t)} - x^{(t_i)}}{\Delta t}$ as the forward difference approximation of x at t_i. The received power difference at time t_i yields

$$\Delta p^{(t_i)} = \Delta y^{(t_i)} + \Delta \psi^{(t_i)}. \tag{15}$$

Considering (12) and $\Delta y^{(t_i)} \approx \frac{dy^{(t)}}{dt}|_{t=t_i}$ yields then

$$\Delta y^{(t_i)} \approx \frac{dl(r)}{dr}|_{r=r_i} \cdot \frac{dr}{dt}|_{t=t_i} + \frac{dg(\beta)}{d\beta}|_{\beta=\beta_i} \cdot \frac{d\beta}{dt}|_{t=t_i} \tag{16}$$

Using (13) and (14), and calculating the derivatives in (16) at given points gives

$$\Delta y^{(t_i)} \approx \frac{v_0}{r_i}\Big(\frac{A_2}{\ln(10)} \cdot \cos(\alpha_0 - \beta_i) - \frac{2B_1}{B_2} \cdot \beta_i \sin(\alpha_0 - \beta_i)\Big). \tag{17}$$

Let Δt be 1 time unit; if the A3 event is triggered at time t_0, we can derive the random variable $\Delta^{(t_0+\tau)} = p_{\text{n}}^{(t_0+\tau)} - p_{\text{s}}^{(t_0+\tau)}, \tau > 0$ in (5) and (7) as follows.

$$\begin{aligned}\Delta^{(t_0+\tau)} =& \Delta^{(t_0)} + \sum_{t=1}^{\tau}(\Delta^{(t_0+t)} - \Delta^{(t_0+t-1)}) \\ =& H + \sum_{t=1}^{\tau}\Big((p_{\text{n}}^{(t_0+t)} - p_{\text{n}}^{(t_0+t-1)}) - (p_{\text{s}}^{(t_0+t)} - p_{\text{s}}^{(t_0+t-1)})\Big) \\ \overset{(15)}{=}& H + M^{(t_0+\tau)} + \Psi^{(t_0+\tau)}\end{aligned} \tag{18}$$

where

$$\begin{aligned}M^{(t_0+\tau)} &= \sum_{t=1}^{\tau}\Big(\Delta y_n^{(t_0+t)} - \Delta y_s^{(t_0+t)}\Big) \\ \Psi^{(t_0+\tau)} &= \sum_{t=1}^{\tau}\Big(\Delta \psi_n^{(t_0+t)} - \Delta \psi_s^{(t_0+t)}\Big)\end{aligned} \tag{19}$$

Note that $M^{(t_0+\tau)}$ in (19) can be calculated by applying (17) (knowing r_0, β_0 at time t_0 and the moving distance $v_0 \cdot t$; with triangular laws we can then calculate β_t and $dist_t$ at time $t_0 + t$). While the sum of the first and second term in (18) is then deterministic, the third term $\Psi^{(t_0+\tau)}$ in (18) is an *unknown random variable*; however, we can assume that $\forall \tau > 0$, it follows a stochastic process with zero mean and variance C, where C can be learned by some machine learning techniques. Thus, the random variable $\Delta^{(t_0+\tau)}$ follows a distribution with the mean $\mu(\Delta^{(t_0+\tau)})$ and the variance $\sigma(\Delta^{(t_0+\tau)})$ given by (8) and (9), respectively.

B. Upperbound of channel outage ratio

By Chebyshev's Inequality to (10), we obtain

$$\begin{aligned}\hat{P}_{\text{out}}^{(t_0+T)} &= \frac{1}{T}\sum_{\tau=1}^{T} Pr\{\Delta^{(t_0+\tau)} > -\Gamma_{\min}\} \\ &= \frac{1}{T}\sum_{\tau=1}^{T} Pr\{\Delta^{(t_0+\tau)} > \frac{\mu + \Gamma_{\min}}{-\sqrt{\sigma}} \cdot \sqrt{\sigma} + \mu\} \\ &\leq \frac{1}{T}\sum_{\tau=1}^{T} \frac{1}{2}\frac{\sigma}{(\mu + \Gamma_{\min})^2} \\ &\overset{(8),(9)}{=} \frac{C}{2T}\sum_{\tau=1}^{T} \frac{1}{(H + M^{(t_0+\tau)} + \Gamma_{\min})^2}\end{aligned}$$

where μ and σ denote the mean and variance of $\Delta^{(t_0+\tau)}$.

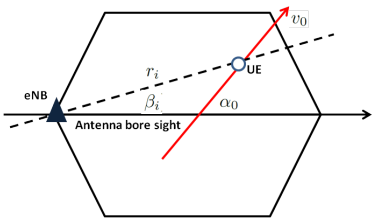

Fig. 5. Change of received power strength due to mobility

C. Upperbound of ping-pong handover ratio

Applying Chebyshev's Inequality to (7) yields

$$\begin{aligned}\hat{P}_{\text{pp}}^{(t_1+T)} &= \prod_{\tau=1}^{T} Pr\{-\Delta^{(t_0+T+\tau)} > H\} \\ &= \prod_{\tau=1}^{T} P\{\Delta^{(t_0+T+\tau)} < \frac{\mu' + H}{-\sqrt{\sigma'}} \cdot \sqrt{\sigma'} + \mu'\} \\ &\leq \prod_{\tau=1}^{T} \frac{1}{2}(\frac{\mu' + H}{-\sqrt{\sigma'}})^{-2} \\ &\overset{(8),(9)}{=} \frac{C}{2}\prod_{\tau=1}^{T} \frac{1}{\big(2H + M^{(t_0+T+\tau)}\big)^2}\end{aligned}$$

where μ' and σ' are the mean and variance of $\Delta^{(t_0+T+\tau)}$.

REFERENCES

[1] O. Sallent, J. Prez-Romero, J. Sanchez-Gonzalez, R. Agust, M. n. Daz-Guerra, D. Henche, and D. Paul, "A roadmap from UMTS optimization to LTE self-optimization." *IEEE Communications Magazine*, vol. 49, no. 6, pp. 172–182, 2011.

[2] 3GPP, *Evolved Universal Terrestrial Radio Access Network (E-UTRAN); Self-configuring and self-optimizing network (SON) use cases and solutions*, 3GPP Std. 36.902 v9.3.1, 2011.

[3] M. Carvalho and P. Vieira, "An enhanced handover oscillation control algorithm in LTE Self-Optimizing networks," in *14th International Symposium on Wireless Personal Multimedia Communications (WPMC), Brest, France, October, 2011*, pp. 1–5.

[4] W. Li, C. Zhang, L. Jin, Z. Wang, L. Zhang, and Y. Liu, "A dynamic maxPRB-Adjusting scheduling scheme based on SINR dispersion degree in LTE System," in *Proceedings of the 75th IEEE Vehicular Technology Conference (VTC) Spring, Yokohama, Japan, May, 2012*, pp. 1–5.

[5] T. Jansen, I. Balan, J. Turk, I. Moerman, and T. Kürner, "Handover parameter optimization in LTE Self-Organizing Networks," in *Proceedings of the 72nd IEEE Vehicular Technology Conference (VTC) Fall, Ottawa, Canada, September 2010*, pp. 1–5.

[6] K. Kitagawa, T. Komine, T. Yamamoto, and S. Konishi, "A handover optimization algorithm with mobility robustness for LTE systems," in *IEEE 22nd International Symposium on Personal, Indoor and Mobile Radio Communications (PIMRC), Toronto, Canada, September, 2011*, pp. 1647–1651.

[7] I. Viering, B. Wegmann, A. Lobinger, A. Awada, and H. Martikainen, "Mobility robustness optimization beyond Doppler effect and WSS assumption," in *8th International Symposium on Wireless Communication Systems (ISWCS), Aachen, Germany, November, 2011*, pp. 186–191.

[8] P. Legg, G. Hui, and J. Johansson, "A simulation study of LTE intra-Frequency handover performance," in *Proceedings of the 72nd IEEE Vehicular Technology Conference (VTC) Fall, Ottawa, Canada, September 2010*, pp. 1–5.

[9] 3GPP, *Evolved Universal Terrestrial Radio Access (E-UTRA); Radio Resource Control (RRC); Protocol specification*, 3GPP Std. 36.331 v11.1.0, 2012.

[10] D. J. Young and N. C. Beaulieu, "The generation of correlated Rayleigh random variates by inverse discrete Fourier transform," *IEEE Transactions on Communications*, vol. 48, no. 7, pp. 1114–1127, 2000.